

# QUBIQ: Uncertainty Quantification for Biomedical Image Segmentation Challenge

Hongwei Bran Li<sup>a,b,c</sup>, Fernando Navarro<sup>a,c,e,i</sup>, Ivan Ezhov<sup>a,i</sup>, Amirhossein Bayat<sup>a</sup>, Dhritiman Das<sup>a,j</sup>, Florian Kofler<sup>ax,a,ay,az</sup>, Suprosanna Shit<sup>a</sup>, Diana Waldmannstetter<sup>a,c</sup>, Johannes C. Paetzold<sup>a</sup>, Xiaobin Hu<sup>a</sup>, Benedikt Wiestler<sup>az</sup>, Lucas Zimmer<sup>c</sup>, Tamaz Amiranashvili<sup>c</sup>, Chinmay Prabhakar<sup>c</sup>, Christoph Berger<sup>a</sup>, Jonas Weidner<sup>a,i</sup>, Michelle Alonso-Basanta<sup>m</sup>, Arif Rashid<sup>m,o</sup>, Ujjwal Baid<sup>n,r</sup>, Wesam Adel<sup>p</sup>, Deniz Alis<sup>q</sup>, Bhakti Baheti<sup>r</sup>, Yingbin Bai<sup>s</sup>, Ishaan Bhat<sup>t</sup>, Sabri Can Cetindag<sup>u</sup>, Wenting Chen<sup>at,v</sup>, Li Cheng<sup>w</sup>, Prasad Dutande<sup>r</sup>, Lara Dular<sup>x</sup>, Mustafa A. Elattar<sup>p</sup>, Ming Feng<sup>y</sup>, Shengbo Gao<sup>z,aa</sup>, Henkjan Huisman<sup>av</sup>, Weifeng Hu<sup>z</sup>, Shubham Innani<sup>r</sup>, Wei Ji<sup>at,w</sup>, Davood Karimi<sup>ab</sup>, Hugo J. Kuijff<sup>t</sup>, Jin Tae Kwak<sup>ac</sup>, Hoang Long Le<sup>ad</sup>, Xiang Li<sup>ae</sup>, Huiyan Lin<sup>af</sup>, Tongliang Liu<sup>s</sup>, Jun Ma<sup>au</sup>, Kai Ma<sup>at</sup>, Ting Ma<sup>ag,ah,ai,aj</sup>, Ilkay Oksuz<sup>u</sup>, Robbie Holland<sup>l</sup>, Arlindo L. Oliveira<sup>ak</sup>, Jimut Bahan Pal<sup>al</sup>, Xuan Pei<sup>z</sup>, Maoying Qiao<sup>am,an</sup>, Anindo Saha<sup>av</sup>, Raghavendra Selvan<sup>ao</sup>, Linlin Shen<sup>v</sup>, Joao Lourenco Silva<sup>ak</sup>, Ziga Spiclin<sup>x</sup>, Sanjay Talbar<sup>r</sup>, Dadong Wang<sup>an</sup>, Wei Wang<sup>af</sup>, Xiong Wang<sup>z</sup>, Yin Wang<sup>y</sup>, Ruiling Xi<sup>af</sup>, Kele Xu<sup>ap,aq</sup>, Yanwu Yang<sup>ag</sup>, Mert Yergin<sup>ar</sup>, Shuang Yu<sup>at</sup>, Lingxi Zeng<sup>af</sup>, YingLin Zhang<sup>af</sup>, Jiachen Zhao<sup>as</sup>, Yefeng Zheng<sup>at</sup>, Martin Zukovec<sup>x</sup>, Richard Do<sup>g</sup>, Anton Becker<sup>g,k</sup>, Amber Simpson<sup>h</sup>, Ender Konukoglu<sup>f</sup>, Andras Jakab<sup>d</sup>, Spyridon Bakas<sup>n</sup>, Leo Joskowicz<sup>aw</sup>, Bjoern Menze<sup>c,a</sup>

<sup>a</sup>Department of Informatics, Technical University of Munich, Germany.

<sup>b</sup>Athinoula A. Martinos Center for Biomedical Imaging, Massachusetts General Hospital, Harvard Medical School, USA.

<sup>c</sup>Department of Quantitative Biomedicine, University of Zurich, Switzerland.

<sup>d</sup>University Children's Hospital Zurich, University of Zurich, Switzerland.

<sup>e</sup>Department of Radioncology and Radiation Therapy, Klinikum rechts der Isar, Technical University of Munich, Germany

<sup>f</sup>Department of Information Technology and Electrical Engineering, ETH-Zurich, Switzerland.

<sup>g</sup>Department of Radiology, Memorial Sloan Kettering Cancer Center in New York City, USA

<sup>h</sup>Department of Biomedical and Molecular Sciences, Queen's University, Canada

<sup>i</sup>TranslaTUM - Central Institute for Translational Cancer Research, Technical University of Munich, Germany

<sup>j</sup>McGovern Institute, Massachusetts Institute of Technology, USA

<sup>k</sup>Institute for Diagnostic and Interventional Radiology, Unveristy Zurich Hospital, Switzerland.

<sup>l</sup>BioMedIA, Imperial College London, United Kingdom.

<sup>m</sup>Department of Radiation Oncology, University of Pennsylvania, PA, USA

<sup>n</sup>University of Pennsylvania, PA, USA

<sup>o</sup>Department of Radiation Oncology, Winship Cancer Institute of Emory University, Georgia, USA

<sup>p</sup>Nile University, Cairo, Egypt

<sup>q</sup>Department of Medical Sciences, Acibadem University, Istanbul, Turkey

<sup>r</sup>Shri Guru Gobind Singhji Institute of Engineering and Technology, Nanded, Maharashtra, India

<sup>s</sup>Trustworthy Machine Learning Lab, University of Sydney, Australia

<sup>t</sup>Image Sciences Institute, University Medical Center Utrecht, The Netherlands

<sup>u</sup>Computer Engineering Department, Istanbul Technical University, Istanbul, Turkey

<sup>v</sup>School of Computer Science, Shenzhen University, Shenzhen, China

<sup>w</sup>University of Alberta, USA

<sup>x</sup>University of Ljubljana, Faculty of Electrical Engineering, Ljubljana, Slovenia

<sup>y</sup>Tongji University, Shanghai, China

<sup>z</sup>OPPO Research Institute, Shanghai, China

<sup>aa</sup>School of Biological and Medical Engineering, Beihang University, Beijing, China

<sup>ab</sup>Harvard Medical School, Boston, USA

<sup>ac</sup>School of Electrical Engineering, Korea University, Seoul, Korea

<sup>ad</sup>Department of Computer Science and Engineering, Sejong University, Seoul, Korea

<sup>ae</sup>Harbin Institute of Technology, China

<sup>af</sup>Southern University of Science and Technology, China

<sup>ag</sup>Department of Electronic and Information Engineering, Harbin Institute of Technology at Shenzhen, China

<sup>ah</sup>Peng Cheng Lab, Shenzhen, China

<sup>ai</sup>Advanced Innovation Center for Human Brain Protection, Capital Medical University, Beijing, China

<sup>aj</sup>National Clinical Research Center for Geriatric Disorders, Xuanwu Hospital Capital Medical University, Beijing, China

<sup>ak</sup>Instituto Superior Tecnico / INESC-ID, Portugal

<sup>al</sup>Department of Computer Science, Ramakrishna Mission Vivekananda Educational and Research Institute, India

<sup>am</sup>Australian Catholic University, Australia

<sup>an</sup>Commonwealth Scientific and Industrial Research Organisation (CSIRO), Australia

<sup>ao</sup>University of Copenhagen, Denmark

<sup>ap</sup>National Key Lab of Parallel and Distributed Processing, Changsha, China

<sup>aq</sup>National University of Defense Technology, Changsha, China

<sup>ar</sup>Hevi AI, Istanbul, Turkey

<sup>as</sup>Department of Computer Science and Engineering, Hongkong University of Science and Technology, China

<sup>at</sup>Tencent Healthcare (Shenzhen) Co., Ltd, China

<sup>au</sup>Department of Mathematics, Nanjing University of Science and Technology, China

<sup>av</sup>Diagnostic Image Analysis Group, Radboud University Medical Center, Nijmegen, The Netherlands

<sup>aw</sup>The Rachel and Selim Benin School of Computer Science and Engineering, The Hebrew University of Jerusalem, Israel

<sup>ax</sup>Helmholtz AI, Helmholtz Zentrum Munchen, Germany

<sup>ay</sup>TranslaTUM - Central Institute for Translational Cancer Research, Technical University of Munich, Germany

<sup>az</sup>Department of Diagnostic and Interventional Neuroradiology, School of Medicine, Klinikum rechts der Isar, Technical University of Munich, Germany

---

## Abstract

Uncertainty in medical image segmentation tasks, especially inter-rater variability, arising from differences in interpretations and annotations by various experts, presents a significant challenge in achieving consistent and reliable image segmentation. This variability not only reflects the inherent complexity and subjective nature of medical image interpretation but also directly impacts the development and evaluation of automated segmentation algorithms. Accurately modeling and quantifying this variability is essential for enhancing the robustness and clinical applicability of these algorithms. We report the set-up and summarize the benchmark results of the Quantification of Uncertainties in Biomedical Image Quantification Challenge (QUBIQ), which was organized in conjunction with International Conferences on Medical Image Computing and Computer-Assisted Intervention (MICCAI) 2020 and 2021. The challenge focuses on the uncertainty quantification of medical image segmentation which considers the omnipresence of inter-rater variability in imaging datasets. The large collection of images with multi-rater annotations features various modalities such as MRI and CT; various organs such as the brain, prostate, kidney, and pancreas; and different image dimensions 2D-vs-3D. A total of 24 teams submitted different solutions to the problem, combining various baseline models, Bayesian neural networks, and ensemble model techniques. The obtained results indicate the importance of the ensemble models, as well as the need for further research to develop efficient 3D methods for uncertainty quantification methods in 3D segmentation tasks.

---

## 1. Introduction

*Background.* The segmentation of anatomical structures and pathologies in medical images frequently encounters substantial inter-rater variability (Lazarus et al., 2006; Watadani et al., 2013), which in turn significantly impacts downstream supervised-learning tasks and clinical decision-making processes. This variability becomes especially pronounced in the context of medical imaging, where manual annotations are often limited and costly to acquire (Kofler et al., 2023). A notable example of this challenge is the segmentation of liver lesions in CT scans, which is inherently complex even for experienced experts, due to the

June 25, 2024

variability in lesion location, contrast, and size among different patients (Joskowicz et al., 2019). It has been observed that the range of variability in manual delineations for various structures and observers is extensive, encompassing a wide spectrum of structures and pathologies, as shown in Figure 1. The involvement of only two or three observers may be inadequate to capture the full breadth of potential variability in the outlines of the targeted structures. This variability, intrinsic to the biological problem, the imaging modality, and the expertise of the annotators has not yet been adequately addressed in the design of computerized algorithms for medical image quantification (Kofler et al., 2021b).

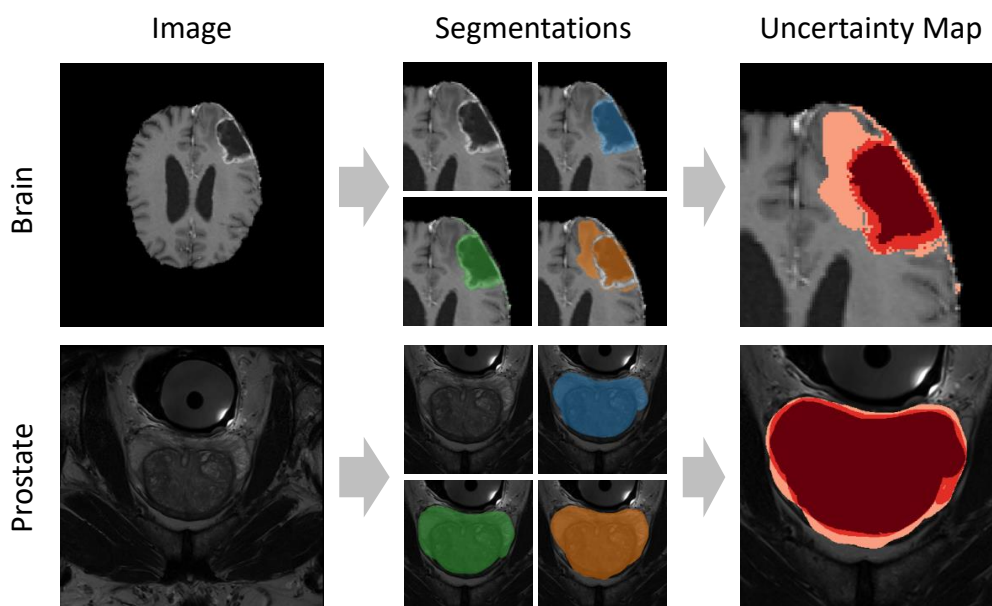


Figure 1: Visualisation of the multi-rater segmentation masks on brain and prostate MRI scans and their derived uncertainty map.

*Uncertainty quantification.* Current methods for modeling uncertainty in predicted image segmentations primarily stem from general statistical model considerations, ensemble approaches involving resampling of training datasets, and aggregating multiple segmentation results, or systematic modifications to the predictive algorithm, as seen in techniques like Monte Carlo (MC) dropout. Yet, the exact delineation of segmented structures within an image inherently carries uncertainty, which is both task-specific and dependent on the dataset. Importantly, this uncertainty can be directly extrapolated from annotations made by multiple human experts. To our knowledge, there are currently no datasets available specifically for evaluating the accuracy of probabilistic model predictions against such multi-expert ground truths. Furthermore, there is a lack of consensus on which uncertainty quantification procedures yield realistic estimates and which do not.

*Objective.* The primary goal of the challenge is to establish a benchmark for algorithms that generate uncertainty estimates (such as probability scores and variability regions) in medical imaging segmentation tasks. The focus is to compare these algorithmic outputs against the uncertainties ascribed by human annotators in the local delineation of structures across various biomedical imaging segmentation tasks. These tasks include, but are not limited to, the segmentation of lesions (such as brain, pancreas, or prostate tumors) and anatomical structures (like brain, kidney, prostate, and pancreas). Multiple expert annotations have been gathered for several CT and MR image datasets to quantify boundary delineation variability.

*Contributions.* In an effort to assess the latest methods in uncertainty quantification for medical image segmentation, we organized the Uncertainty Quantification of Biomedical Image Quantification Challenge (QUBIQ) at MICCAI-2020 and MICCAI-2021. This paper highlights three major contributions to this field. Firstly, we introduce a new, publicly available multi-rater, multi-center, multi-modality dataset that includes both 2D and 3D segmentation tasks. Secondly, we present the setup and summarize the findings of our QUBIQ uncertainty quantification benchmarks held at two grand challenges. Lastly, we review, evaluate, rank, and analyze the state-of-the-art algorithms that emerged from these benchmarks.

## 2. Prior Work on Approaches and Datasets

### 2.1. Prior work.

There is a body of literature that models uncertainty and inter-rater variability in biomedical image segmentation (Lê et al., 2016; Sabuncu et al., 2010; Kwon et al., 2020; Roy et al., 2019; Ilg et al., 2018). Some of the prior methods directly extract uncertainty estimates from trained models, either by augmenting the input image Wang et al. (2019) or by generating multiple potential segmentations using MC dropout Nair et al. (2020). Others modify techniques into ensemble methods that generate multiple parallel predictions Ilg et al. (2018) or by running multiple models in parallel Calisto & Lai-Yuen (2020). Kofler et al. (2021a) extend this further to create an ensemble of multiple approaches from the literature and create a system to alert the user if there is low segmentation agreement within the ensemble. In contrast, others explicitly model inter-rater uncertainty. In Probabilistic U-Net, Kohl et al. Kohl et al. (2018) use variational inference to learn a prior distribution of variability, from which they sample plausible segmentations, while Baumgartner et al. Baumgartner et al. (2019) extend this to a hierarchical model capable of modeling uncertainty at different levels of abstraction within the U-Net architecture. Monteiro et al. Monteiro et al. (2020) explicitly model uncertainty by learning a low-rank pixel-wise covariance matrix.

### 2.2. Publicly available datasets.

Table 1 showcases available datasets for uncertainty quantification task. Most of the datasets feature multi-rater labeling. Each focuses on a particular pathological or healthy anatomy segmentation task.

Therefore, the datasets either contain 2D or 3D images, CT or MRI modality. The QUBIQ challenge offers a dataset composed of multiple tasks for both image dimensions and imaging modalities.

Table 1: Overview of publicly available medical datasets for uncertainty quantification in image segmentation tasks. (to be updated)

Dataset	Modality	Target	2D	3D	#Images	multi-rater
LIDC-IDRI (Armato III et al., 2011)	CT	Lung nodule	✓	✗	1,018	✓
MICCAI-2012 (Litjens et al., 2012)	MRI	Prostate	✓	✗	48	✓
ISBI-2015 (Styner et al., 2008)	MRI	MS lesion	✗	✓	21	✓
BraTS (Mehta et al., 2020)	MRI	brain tumor	✗	✓	335	✗
<b>QUBIQ</b>	CT,MRI	<b>six tasks</b>	✓	✓	**	✓

### 3. QUBIQ challenge

#### 3.1. QUBIQ datasets

##### 3.1.1. Dataset creation.

For the adult glioma segmentation task, we employ three label sets. The first label set is the original label from the BraTS adult glioma segmentation challenge (Bakas et al., 2019). Additionally, we use two algorithm-based labels obtained from BraTS Toolkit (Kofler et al., 2020). To generate these, we first generate five algorithmic (Isensee et al., 2019; McKinley et al., 2019; Feng et al., 2020,?; Zhao et al., 2019; McKinley et al., 2020) glioma segmentations. Subsequently, we fuse these using basic majority voting and SIMPLE fusion (Langerak et al., 2010).

Table 2: Overview of QUBIQ datasets and the sub-tasks

Dataset	Modality	[2020,2021]	2D	3D	#Images	#Tasks	Source (NEED to double check)
Prostate segmentation	MRI	[✓,✓]	✓	✗	55	2	ETH Zrich
Brain growth segmentation	MRI	[✓,✓]	✓	✗	39	1	University of Zrich
Brain tumor segmentation	multimodal MRI	[✓,✓]	✓	✗	32	3	University of Pennsylvania
Kidney segmentation	CT	[✓,✓]	✓	✗	24	1	Technical University of Munich
Pancreas segmentation	CT	[✗,✓]	✗	✓	38	1	University of Pennsylvania
Pancreatic lesion segmentation	CT	[✗,✓]	✗	✓	21	1	University of Pennsylvania

#### 3.2. Evaluation metrics and ranking

For the evaluation, each participant had to segment the given binary structures and predict the distribution of the experts’ labels by returning one mask with continuous values between 0 and 1 which is supposed to reproduce the average segmentations of the experts.

Predictions and continuous ground truth labels are compared by thresholding the continuous labels at predefined thresholds and calculating the volumetric overlap of the resulting binary volumes using the Dice

score (the continuous ground truth labels are obtained by averaging multiple experts’ annotations). To this end, both the ground truth and prediction are binarized at ten probability levels (0.1, 0.2, ..., 0.8, 0.9). Dice scores for all thresholds are averaged.

The Q-Dice, a staged Dice score, is used to quantify the quality of the predicted probability map  $p$  against the ground truth  $y$  in  $L$  discrete probability levels, formulated as:

$$T_L(p, l) = \begin{cases} \mathbb{1} \left\{ \frac{l}{L} \leq p < \frac{l+1}{L} \right\}, & \text{if } 0 \leq l < L - 1 \\ \mathbb{1} \left\{ \frac{l}{L} \leq p \leq \frac{l+1}{L} \right\}, & \text{if } l = L - 1 \end{cases} \quad (1)$$

Compared to the original Dice score, Q-score quantifies the uncertainty by comparing the prediction and ground truth maps at different confidence levels. Since in most cases experts agree on most parts of the annotations, the variance of different Q-score demonstrates how well the prediction modeled the uncertainty on the borders of the structure of interest.

### 3.3. Challenge events

The QUBIQ challenge was organized within the MICCAI conference using the Grand Challenge platform. Below in Tables 3, 4, and 5, we provide descriptions of algorithms across the two iterations of the QUBIQ challenge (QUBIQ2020 and QUBIQ2021). Fig. 2 quantitatively compares the algorithms over the two iterations of the challenge.

### 3.4. Results

In Tables 3 and 4, we show the leaderboard for both iterations of the challenge.

Table 3: Results QUBIQ 2020 ordered according to the ranking score. The top 3 performing teams are highlighted in blue color. Notice that only teams participating in all tasks are considered for the overall ranking.

Ref. Name	Brain-growth	Brain-tumor	Brain-tumor	Brain-tumor	Kidney	Prostate	Prostate	Average	Average
		Task 1	Task 2	Task 3		Task 1	Task 2	Ranking	Dice
■ Jun_Ma	<b>0.921</b>	<b>0.936</b>	<b>0.809</b>	0.822	0.310	<b>0.970</b>	<b>0.918</b>	<b>7.857</b>	0.812
■ Yanwu_Yang	0.893	0.917	0.699	<b>0.836</b>	0.825	0.937	0.878	7.143	<b>0.855</b>
Macaroon	0.878	0.848	0.528	0.690	0.238	0.937	0.890	5	0.715
■ Raghavendra_Selvan 2	0.885	0.899	0.617	0.682	0.695	0.883	0.800	4.857	0.780
■ Raghavendra_Selvan	0.907	0.874	0.602	0.690	0.639	0.858	0.780	4.714	0.764
■ Wei_Ji	0.900	0.755	0.323	0.605	0.915	0.941	0.845	4.714	0.755
■ Xiang_Li	0.865	0.931	0.513	0.556	0.903	0.914	0.872	4.714	0.793
■ Ujjwal_Baid	0.840	0.782	0.406	0.568	<b>0.956</b>	0.891	0.702	3.143	0.735
Maykol_Campos	0.849	0.799	0.522	0.613	0.805	0.838	0.630	2.857	0.722
anysys99	0.818	0.893	0.485	0.724	-	0.890	0.804	-	-
■ Davood_Karimi	0.874	0.900	0.452	-	0.785	0.947	0.897	-	-

Table 4: Results QUIBIQ 2021 ordered according to the ranking score. The top 3 performing teams are highlighted in blue color. Notice that only teams participating in all tasks are considered for the overall ranking.

Team	Brain-growth	Brain-tumor	Brain-tumor	Brain-tumor	Kidney	Prostate	Prostate	Pancreas	Pancreatic	Average	Average
		Task 1	Task 2	Task 3		Task 1	Task 2		Lesion	Ranking	Dice
Peng-Cheng_Shi	0.929	0.938	0.819	0.847	<b>0.954</b>	0.969	0.920	0.550	0.272	<b>11.111</b>	<b>0.800</b>
■ Yingbin_Bai	0.915	0.928	0.793	0.815	0.940	0.968	0.920	0.579	0.205	9.333	0.785
■ Lara_Dular	0.928	0.938	<b>0.820</b>	<b>0.899</b>	0.467	0.958	0.909	0.499	0.283	8.778	0.745
■ Lawrence_Schobs	0.300	0.939	0.780	0.798	0.503	0.969	0.915	<b>0.683</b>	<b>0.330</b>	8.556	0.691
■ Sabrican_Cetindag	0.928	0.932	0.769	0.883	0.839	0.964	0.922	0.409	0.231	8.444	0.764
■ Yucong_Chen	0.916	0.927	0.775	0.840	0.952	0.952	0.907	0.572	0.130	7.889	0.775
■ Hoang_Long_Le	0.912	0.899	0.680	0.754	0.706	<b>0.971</b>	<b>0.927</b>	0.575	0.246	7.444	0.741
■ Dewen_Zeng	0.927	<b>0.940</b>	0.695	0.835	0.894	0.947	0.911	0.423	0.126	7.111	0.744
■ Joao_Lourenco_Silva	<b>0.931</b>	0.929	0.750	0.797	0.511	0.968	0.920	0.075	0.068	6.333	0.661
■ Anindo_Saha	0.892	0.917	0.695	0.740	0.950	0.936	0.859	0.546	0.194	5.222	0.748
■ Wang_Xiong	0.893	0.905	0.589	0.784	0.930	0.916	0.862	0.557	0.204	5.222	0.738
■ Ishaan_Rajesh	0.892	0.919	0.638	0.704	0.858	0.861	0.799	0.316	0.122	3.111	0.679
■ Stephan_Huschauer	0.719	0.865	0.525	0.551	0.856	0.911	0.842	0.423	0.118	2.444	0.646
■ Jiachen_Zhao	0.873	0.844	0.547	0.787	0.835	0.931	0.884	-	-	-	-
■ Jimut_Bahan_Pal	0.869	0.842	0.456	0.690	0.769	0.833	0.781	-	-	-	-
■ Mohammad_Eslami	0.848	0.404	0.377	0.236	0.716	0.883	0.816	-	-	-	-
■ Shengbo_Gao	0.802	0.885	0.627	0.661	0.910	-	-	0.557	0.130	-	-
■ Xiaofeng_Liu	0.800	-	-	-	-	-	-	-	-	-	-
■ Timothy_S	0.780	-	-	-	-	-	-	-	-	-	-

## 4. Conclusion

In this paper, we report on the results of the QUBIQ challenge (Quantification of Uncertainties in Biomedical Image Quantification Challenge), which was organized in conjunction with International Conferences on Medical Image Computing and Computer-Assisted Intervention (MICCAI). Quantifying uncertainty in medical imaging is paramount for image analysis, as inter-rater variability is omnipresent in imaging datasets. Such quantification could reduce barriers to adopting learnable algorithms into clinical practice. With the QUBIQ challenge, we aim to fill the empty space among the medical imaging challenges, which are dominated by competition in deterministic segmentation, ignoring the importance of uncertainty prediction.

## Acknowledgement

The research is supported through the SFB 824, subproject B12, as well as by Deutsche Forschungsgemeinschaft (DFG) via TUM International Graduate School of Science and Engineering (IGSSE), GSC 81. We acknowledge support by the Helmut Horten Foundation and by the Translational Brain Imaging Training Network (TRABIT) under the EU Horizon 2020 research & innovation program (Grant agreement ID: 765148). Research reported in this publication was partly supported by the National Institutes of Health (NIH) under award numbers NIH/NCI:U01CA242871 and NIH/NINDS:R01NS042645.

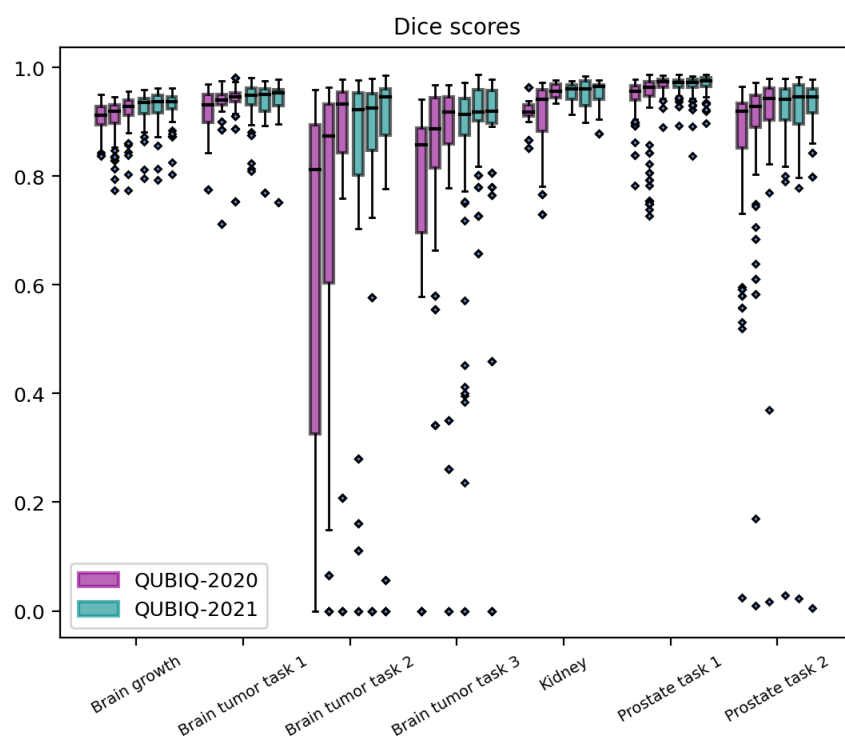


Figure 2: Pictorial evaluation of QUBIQ challenge for different tasks over two years. Observe that for every task, the top-performing methods produce higher scores in 2021 than in 2020. Also, the methods in 2021 are more competitive than in 2020.



Table 5: Details of the participating teams methods in QUBIQ-Challenge-2020.

Lead Author & Team Members	Method, Architecture & Modifications	Data Augmentation	Loss Function	Pre-processing	Label Processing	Ensemble strategy
■ Jun Ma	Multiple 2D U-Nets (one per annotator).	None	Cross-entropy & Dice loss	None	None	Averaging
■ Davood Karimi	2D U-Net with additional connections between coarse and fine feature layers in the encoder. Dynamic loss weighting for harder classes. Multi-task training approach.	None	1-Dice similarity loss	Zero mean, unit variance standardization.	Averaging annotations	None
■ Ming Feng; Kele Xu, Yin Wang	2D U-Net trained with ground truth & predictions binarized at different levels, averaging Dice score of each prediction.	Random scaling [0.9, 1.1]	Weighted cross-entropy & Dice loss	Resizing to 256 × 256 (brain tumor) 512 × 512 (kidney & prostate). Normalization to [0, 255].	Averaging annotations	None
■ Raghavendra Selvan	Multi-channel U-Net, one channel for each rater. Based on concept of Normalizing Flows.	None	Planar Flow & Dice loss	None	None	None
■ Ujjwal Baid; Prasad Dutande, Shubham Innani, Bhakti Baheti, Sanjay Talbar	ResNet34 based encoder-decoder. Different annotations included as individual copies in training set.	Rotation, flip & scaling	None	Resizing to 256 × 256 (brain) 512 × 512 (kidney) 640 × 640 (prostate).	None	None
■ Wesam Adel; Mustafa A. Elattar	2D U-Net trained with averaged annotations and as a regression problem.	None	Weighted KL-divergence	Resizing brain to 256 × 256 with rotation and elastic deformation.	None	None
■ Xiang Li	U Net with attention, 4x downsampling for Kidney and 5x for others.	None	Weighted cross-entropy	Cropping to 128 × 128 (kidney) 416 × 416 (prostate)	Averaging annotations	None
■ Yanwu Yang; Ting Ma	2D U-Net with multiple branches. Instance Norm instead of Batch Norm. One model per annotation integrated using auxiliary loss.	None	Cross-entropy & Dice loss	MRI: z-score normalization. CT: centering on ROI and rescaling to [0, 1]	None	Averaging
■ Wei Ji; Wenting Chen Shuang Yu Kai Ma Li Cheng Linlin Shen Yefeng Zheng	U-Net with Resnet-34 encoder. One output channel per label and one model per annotation integrated using auxiliary loss.	None	Cross-entropy	Resizing to 512 × 512	Both fused final & individual labels. Combining labels via averaging, random sampling & label sampling.	Weighted average

Table 6: Details of the participating teams methods in QUBIQ-Challenge-2021 (part 1).

Lead Author & Team Members	Method, Architecture & Modifications	Data Augmentation	Loss Function	Pre-processing	Label Processing	Ensemble strategy
■ Anindo Saha; Henkjan Huisman	Probabilistic U-Net with MC Dropout.	Gaussian noise, horizontal flip, rotation, translation & scaling	KL-Divergence & Dice loss	z-Score normalization, centre cropping to 512 × 512 (Kidney) 256 × 256 (Brain) 640 × 640 (Prostrate)	None	Deep ensemble (averaging)
■ Hoang Long Le; Jin Tae Kwak	DeepLabv3 & EfficientNet (latter for classifying pancreas existence). 9 binary ground truths from thresholding.	Gaussian noise, horizontal & vertical flip, rotation, shift scaling, blur random brightness	Dice loss	Normalization to [0, 255]	Averaging annotations	Multiplying binary segmentation map with threshold value & taking per pixel maximum.
■ Ishaan Bhat; Hugo J. Kuijff	Probabilistic U-Net with MC Dropout.	Random flip, rotation, brightness & contrast	Cross-entropy & KL-Divergence	z-Score normalization, Resizing to 256 × 256 (brain) 512 × 512 (kidney) 512 × 512 (pancreas)	None	Deep ensemble (averaging)
■ Jiachen Zhao	U-Net	Random flip	Dice loss	Resizing to 256 × 256	Averaging annotations	None
■ Jimut Bahan Pal	Multiple U-Nets (one per annotation).	None	Focal Tversky	None	None	None
■ João Lourenço Silva; Arlindo L. Oliveira	U-Net with EfficientNet-B0 encoder.	Rotation, horizontal & vertical flip, translation & zoom	Cross-entropy	None	Averaging annotations	None
■ Lawrence Schobs	Multiple nnU-Nets (one per annotator, 2D for pancreas, 3D for other).	Gaussian noise, rotation, scaling mirroring & inhomogeneity	Dice loss	Resizing prostate images to 640 × 640. Image sampling and normalization.	Averaging annotations	None
■ Martin Žukovec; Lara Dular Žiga Špiclin	nnU-Net. Multi-task training approach with labels 0–N (N annotators + background).	Gaussian noise, rotation, scaling mirroring & inhomogeneity	Dice loss	Image sampling and normalization	Addition of segmentations	None
■ Sabri Can Cetindag; Mert Yergin Deniz Alis Ilkay Oksuz	nnU-Net, training one U-Net per annotator, then adding segmentation map output as extra channels.	None	Cross-entropy & Dice loss	None	Average of annotations for stage 2	None
■ Xiong Wang; Shengbo Gao Weifeng Hu Xuan Pei	2D: U-Net (one per annotator, obtained via label fusion), MaskNet, and DeepLab V3+. 3D: SegResNet.	None	Weighted focal & Dice loss	None	Label fusion for training individual models	Weighted combination
■ YingLin Zhang; Wei Wang Ruiling Xi Lingxi Zeng Huiyan Lin	UNet, UNet++, and TransUNet.	Gaussian noise, horizontal & vertical flip, rotation, translation, zoom, brightness, sharpness, contrast, blur & elastic deformation	Multi-level Dice loss	Center-cropping images to ROI. Discarding images with unclear ROI	Majority voting, cumulative division & even division of segmentations	Weighted combination
■ Yingbin Bai; Maoying Qiao Dadong Wang Tongliang Liu	UNet++ with EfficientNet-B7 encoder.	None	Multi-level Dice loss	None	Weighted combination of individual segmentation maps	None

Table 7: Details of the participating teams methods in QUBIQ-Challenge-2021 (part 2).

Lead Author & Team Members	Method, Architecture & Modifications	Data Augmentation	Loss Function	Pre-processing	Label Processing	Ensemble strategy
■ Dewen Zeng; Yukun Ding Yiyu Shi	2D U-Net with multiple loss functions (one each for individual annotators, aggregated label & multi-scale threshold).	None	Cross-entropy	z-Score normalization, resizing	Averaging annotations	None
■ Yanwu Yang; Xutao Guo Yiwei Pan Pengcheng Shi Haiyan Lv Ting Ma	2D U-Net with one decoder per annotator and Layer Norm and skip-connections.	None	Cross-entropy & Dice loss on individual decoders A cross loss between different decoders & an auxiliary loss between average prediction & average ground truth	z-Score normalization, resizing	Averaging different labels	Deep ensemble (averaging)
■ Stephan Huschauer	High-Resolution Network (HRNet) with stem layers replaced by 2D wavelet scattering transformation.	None	None	Resizing to $512 \times 512$	Averaging annotations	Deep ensemble (averaging)
■ Xiaofeng Liu; Fangxu Xing Georges El Fakhri Jonghye Woo	Variational Inference encoding multi-annotator variability with a latent variable model.	None	Cross-entropy & L2 reconstruction loss	None	Averaging annotations	Deep ensemble (averaging)
■ Yucong Chen; Guanqi He Zhitong Gao Xuming He	2D U-Net with multiple decoders, one for each annotator.	Random cropping (training), sliding window (inference)	None	None	None	Deep ensemble (averaging)
■ Mohammad Eslami; Farzin Soleymani Anirudh Ashok Bernd Bischl Mina Rezaei	Uncertainty-aware progressive GAN. Encoder modeled using 2D U-Net & Patch Discriminators from Pix2Pix	None	Multi-stage GAN loss and Soft Dice loss	Intensity values normalized between 0-255	Averaging annotations	None
■ Timothy Sum Hon Mun; Simon J Doran Paul Huang Christina Messiou Matthew D Blackledge	2D U-Net with Monte Carlo dropout.	None	Dice loss	None	None	None

## References

- Armato III, S. G., McLennan, G., Bidaut, L., McNitt-Gray, M. F., Meyer, C. R., Reeves, A. P., Zhao, B., Aberle, D. R., Henschke, C. I., Hoffman, E. A. et al. (2011). The lung image database consortium (lidc) and image database resource initiative (idri): a completed reference database of lung nodules on ct scans. *Medical physics*, *38*, 915–931.
- Bakas, S., Reyes, M., Jakab, A., Bauer, S., Rempfler, M., Crimi, A., Shinohara, R. T., Berger, C., Ha, S. M., Rozycki, M., Prastawa, M., Alberts, E., Lipkova, J., Freymann, J., Kirby, J., Bilello, M., Fathallah-Shaykh, H., Wiest, R., Kirschke, J., Wiestler, B., Colen, R., Kotrotsou, A., Lamontagne, P., Marcus, D., Milchenko, M., Nazeri, A., Weber, M.-A., Mahajan, A., Baid, U., Gerstner, E., Kwon, D., Acharya, G., Agarwal, M., Alam, M., Albiol, A., Albiol, A., Albiol, F. J., Alex, V., Allinson, N., Amorim, P. H. A., Amrutkar, A., Anand, G., Andermatt, S., Arbel, T., Arbelaez, P., Avery, A., Azmat, M., B., P., Bai, W., Banerjee, S., Barth, B., Batchelder, T., Batmanghelich, K., Battistella, E., Beers, A., Belyaev, M., Bendszus, M., Benson, E., Bernal, J., Bharath, H. N., Biros, G., Bisdas, S., Brown, J., Cabezas, M., Cao, S., Cardoso, J. M., Carver, E. N., Casamitjana, A., Castillo, L. S., Cat, M., Cattin, P., Cerigues, A., Chagas, V. S., Chandra, S., Chang, Y.-J., Chang, S., Chang, K., Chazalon, J., Chen, S., Chen, W., Chen, J. W., Chen, Z., Cheng, K., Choudhury, A. R., Chylla, R., Clrigues, A., Coleman, S., Colmeiro, R. G. R., Combalia, M., Costa, A., Cui, X., Dai, Z., Dai, L., Daza, L. A., Deutsch, E., Ding, C., Dong, C., Dong, S., Dudzik, W. et al. (2019). Identifying the best machine learning algorithms for brain tumor segmentation, progression assessment, and overall survival prediction in the brats challenge.
- Baumgartner, C. F., Tezcan, K. C., Chaitanya, K., Hötker, A. M., Muehlematter, U. J., Schawkat, K., Becker, A. S., Donati, O., & Konukoglu, E. (2019). Phiseg: Capturing uncertainty in medical image segmentation. In *Medical Image Computing and Computer Assisted Intervention—MICCAI 2019: 22nd International Conference, Shenzhen, China, October 13–17, 2019, Proceedings, Part II 22* (pp. 119–127). Springer.
- Calisto, M. B., & Lai-Yuen, S. K. (2020). Adaen-net: An ensemble of adaptive 2d–3d fully convolutional networks for medical image segmentation. *Neural Networks*, *126*, 76–94.
- Feng, X., Tustison, N. J., Patel, S. H., & Meyer, C. H. (2020). Brain tumor segmentation using an ensemble of 3d u-nets and overall survival prediction using radiomic features. *Frontiers in computational neuroscience*, *14*, 25.
- Ilg, E., Cicek, O., Galesso, S., Klein, A., Makansi, O., Hutter, F., & Brox, T. (2018). Uncertainty estimates and multi-hypotheses networks for optical flow. In *Proceedings of the European Conference on Computer Vision (ECCV)* (pp. 652–667).
- Isensee, F., Kickingereder, P., Wick, W., Bendszus, M., & Maier-Hein, K. H. (2019). No new-net. In *Brainlesion: Glioma, Multiple Sclerosis, Stroke and Traumatic Brain Injuries: 4th International Workshop, BrainLes 2018, Held in Conjunction with MICCAI 2018, Granada, Spain, September 16, 2018, Revised Selected Papers, Part II 4* (pp. 234–244). Springer.
- Joskowicz, L., Cohen, D., Caplan, N., & Sosna, J. (2019). Inter-observer variability of manual contour delineation of structures in ct. *European radiology*, *29*, 1391–1399.
- Kofler, F., Berger, C., Waldmannstetter, D., Lipkova, J., Ezhov, I., Tetteh, G., Kirschke, J., Zimmer, C., Wiestler, B., & Menze, B. H. (2020). Brats toolkit: translating brats brain tumor segmentation algorithms into clinical and scientific practice. *Frontiers in neuroscience*, (p. 125).
- Kofler, F., Ezhov, I., Fidon, L., Pirkl, C. M., Paetzold, J. C., Burian, E., Pati, S., El Hussein, M., Navarro, F., Shit, S. et al. (2021a). Robust, primitive, and unsupervised quality estimation for segmentation ensembles. *Frontiers in Neuroscience*, *15*, 752780.
- Kofler, F., Ezhov, I., Isensee, F., Balsiger, F., Berger, C., Koerner, M., Paetzold, J., Li, H., Shit, S., McKinley, R. et al. (2021b). Are we using appropriate segmentation metrics? identifying correlates of human expert perception for cnn training beyond rolling the dice coefficient. *arXiv preprint arXiv:2103.06205*, .
- Kofler, F., Wahle, J., Ezhov, I., Wagner, S. J., Al-Maskari, R., Gryska, E., Todorov, M., Bukas, C., Meissen, F., Peng, T. et al. (2023). Approaching peak ground truth. In *2023 IEEE 20th International Symposium on Biomedical Imaging (ISBI)* (pp. 1–6). IEEE.

- Kohl, S., Romera-Paredes, B., Meyer, C., De Fauw, J., Ledsam, J. R., Maier-Hein, K., Eslami, S., Jimenez Rezende, D., & Ronneberger, O. (2018). A probabilistic u-net for segmentation of ambiguous images. *Advances in neural information processing systems*, 31.
- Kwon, Y., Won, J.-H., Kim, B. J., & Paik, M. C. (2020). Uncertainty quantification using bayesian neural networks in classification: Application to biomedical image segmentation. *Computational Statistics & Data Analysis*, 142, 106816.
- Langerak, T. R., van der Heide, U. A., Kotte, A. N., Viergever, M. A., Van Vulpen, M., & Pluim, J. P. (2010). Label fusion in atlas-based segmentation using a selective and iterative method for performance level estimation (simple). *IEEE transactions on medical imaging*, 29, 2000–2008.
- Lazarus, E., Mainiero, M. B., Schepps, B., Koelliker, S. L., & Livingston, L. S. (2006). Bi-rads lexicon for us and mammography: interobserver variability and positive predictive value. *Radiology*, 239, 385–391.
- Lê, M., Unkelbach, J., Ayache, N., & Delingette, H. (2016). Sampling image segmentations for uncertainty quantification. *Medical image analysis*, 34, 42–51.
- Litjens, G., Debats, O., van de Ven, W., Karssemeijer, N., & Huisman, H. (2012). A pattern recognition approach to zonal segmentation of the prostate on mri. In *International Conference on Medical Image Computing and Computer-Assisted Intervention* (pp. 413–420). Springer.
- McKinley, R., Meier, R., & Wiest, R. (2019). Ensembles of densely-connected cnns with label-uncertainty for brain tumor segmentation. In *Brainlesion: Glioma, Multiple Sclerosis, Stroke and Traumatic Brain Injuries: 4th International Workshop, BrainLes 2018, Held in Conjunction with MICCAI 2018, Granada, Spain, September 16, 2018, Revised Selected Papers, Part II 4* (pp. 456–465). Springer.
- McKinley, R., Rebsamen, M., Meier, R., & Wiest, R. (2020). Triplanar ensemble of 3d-to-2d cnns with label-uncertainty for brain tumor segmentation. In *Brainlesion: Glioma, Multiple Sclerosis, Stroke and Traumatic Brain Injuries: 5th International Workshop, BrainLes 2019, Held in Conjunction with MICCAI 2019, Shenzhen, China, October 17, 2019, Revised Selected Papers, Part I 5* (pp. 379–387). Springer.
- Mehta, R., Filos, A., Gal, Y., & Arbel, T. (2020). Uncertainty evaluation metric for brain tumour segmentation. *arXiv preprint arXiv:2005.14262*, .
- Monteiro, M., Le Folgoc, L., Coelho de Castro, D., Pawlowski, N., Marques, B., Kamnitsas, K., van der Wilk, M., & Glocker, B. (2020). Stochastic segmentation networks: Modelling spatially correlated aleatoric uncertainty. *Advances in Neural Information Processing Systems*, 33, 12756–12767.
- Nair, T., Precup, D., Arnold, D. L., & Arbel, T. (2020). Exploring uncertainty measures in deep networks for multiple sclerosis lesion detection and segmentation. *Medical image analysis*, 59, 101557.
- Roy, A. G., Conjeti, S., Navab, N., Wachinger, C., Initiative, A. D. N. et al. (2019). Bayesian quicknat: Model uncertainty in deep whole-brain segmentation for structure-wise quality control. *NeuroImage*, 195, 11–22.
- Sabuncu, M. R., Yeo, B. T., Van Leemput, K., Fischl, B., & Golland, P. (2010). A generative model for image segmentation based on label fusion. *IEEE transactions on medical imaging*, 29, 1714–1729.
- Styner, M., Lee, J., Chin, B., Chin, M., Commowick, O., Tran, H., Markovic-Plese, S., Jewells, V., & Warfield, S. (2008). 3d segmentation in the clinic: A grand challenge ii: Ms lesion segmentation. *Midas Journal*, 2008, 1–6.
- Wang, G., Li, W., Aertsen, M., Deprest, J., Ourselin, S., & Vercauteren, T. (2019). Aleatoric uncertainty estimation with test-time augmentation for medical image segmentation with convolutional neural networks. *Neurocomputing*, 338, 34–45.
- Watadani, T., Sakai, F., Johkoh, T., Noma, S., Akira, M., Fujimoto, K., Bankier, A. A., Lee, K. S., Müller, N. L., Song, J.-W. et al. (2013). Interobserver variability in the ct assessment of honeycombing in the lungs. *Radiology*, 266, 936–944.
- Zhao, Y.-X., Zhang, Y.-M., Song, M., & Liu, C.-L. (2019). Multi-view semi-supervised 3d whole brain segmentation with a self-ensemble network. In *Medical Image Computing and Computer Assisted Intervention–MICCAI 2019: 22nd International Conference, Shenzhen, China, October 13–17, 2019, Proceedings, Part III 22* (pp. 256–265). Springer.